

Formally Verifying Quantum Phase Estimation Circuits with 1,000+ Qubits

Arun Govindankutty, Sudarshan K. Srinivasan

Electrical and Computer Engineering Department, North Dakota State University, Fargo, ND, USA

Abstract—We present a scalable formal verification methodology for Quantum Phase Estimation (QPE) circuits. Our approach uses a symbolic qubit abstraction based on quantifier-free bit-vector logic, capturing key quantum phenomena, including superposition, rotation, and measurement. The proposed methodology maps quantum circuit functional behaviour from Hilbert space to a bit-vector domain. We develop formal properties aligned with this abstraction to ensure functional correctness of QPE circuits. The method scales efficiently, verifying QPE circuits with up to 6 precision qubits and 1,024 phase qubits using under 3.5 GB of memory.

Index Terms—formal verification, quantum computing, quantum circuit verification, quantum phase estimation.

I. INTRODUCTION

Quantum computing has demonstrated the potential to surpass classical computation in several classes of problems across domains such as communication, machine learning, materials science, medicine, and optimization, enabling progress toward quantum advantage [1]–[3]. Central to many of these advances are quantum algorithms that address problems intractable for classical systems. Among them, Quantum Phase Estimation (QPE) is a core primitive, employed in key applications including Shor’s algorithm [4], quantum counting and amplitude amplification [5], eigenvalue estimation [6], and quantum linear system solvers [7]. Realizing these applications in practice requires QPE circuits to scale to thousands of qubits. However, increasing circuit scale also amplifies design and functional complexity, significantly raising the risk of implementation errors. Therefore, establishing the functional correctness of large-scale QPE circuits is a critical requirement for reliable quantum computation.

Quantum circuits operate over complex Hilbert spaces and exhibit uniquely quantum effects such as superposition, entanglement, and measurement, making functional verification inherently challenging. Formal verification is well suited to uncover subtle design errors while ensuring design correctness [8]. Recent work has extended these techniques to the quantum domain by adapting classical formal methods to reason about quantum program behavior [9], [10].

This work explicitly incorporates measurement into the abstraction framework to the work presented in [11], yielding a generic symbolic qubit abstraction based on quantifier free bit-vector logic. The resulting model enables functional correctness verification using Satisfiability Modulo Theories (SMT) solvers. Our main contributions are as follows:

- A unified qubit abstraction integrating rotational, superposition, and measurement operations.
- Symbolic abstract modelling of controlled modular exponentiation in QPE circuits.
- Formal specification of correctness properties capturing QPE functionality.
- Soundness lemmas and formal proofs of the proposed verification methodology.

The required theoretical background is presented next.

II. BACKGROUND

This section briefly reviews qubits, quantum gates, and Quantum Phase Estimation (QPE). Detailed treatments can be found in [12]–[14]. The basic unit of quantum information is the qubit, represented as a linear combination of the computational basis states $|0\rangle$ and $|1\rangle$, defined as

$$|0\rangle = \begin{bmatrix} 1 \\ 0 \end{bmatrix}, \quad |1\rangle = \begin{bmatrix} 0 \\ 1 \end{bmatrix}. \quad (1)$$

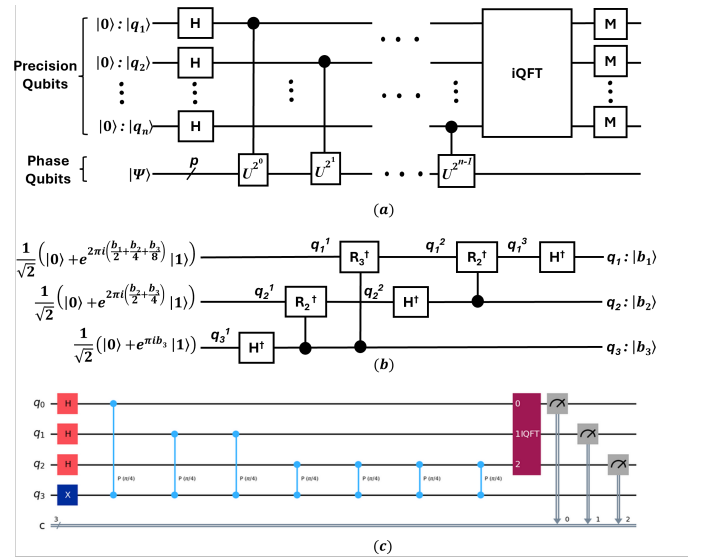


Fig. 1. (a) Quantum phase estimation circuit. (b) 3-qubit inverse quantum Fourier transform circuit [11]. (c) Quantum phase estimation circuit with 3 precision qubits and 1 phase qubit implemented in IBM-Qiskit.

Quantum gates are unitary operators that act on qubits to transform their states. Given a unitary operator U , an eigenstate $|\psi\rangle$, and n precision (ancilla) qubits, a QPE circuit estimates the phase θ with precision $1/2^n$, where

$$U|\psi\rangle = e^{2\pi i\theta}|\psi\rangle. \quad (2)$$

This paper is based upon work supported by the National Science Foundation under Grant No. 2513276.

Figure 1(a) shows a standard QPE circuit [12]. The circuit consists of Hadamard (H) gates to create equal superposition, controlled modular exponentiation operators $C-U^{2^k}$, the inverse Quantum Fourier Transform (iQFT), and measurement (M). As illustrated in Figure 1(b), the iQFT is composed of inverse Hadamard (H^\dagger) and inverse controlled-rotation ($C-R_k^\dagger$) gates. The specific form of $C-U^{2^k}$ depends on the target application. In this work, we assume a generic unitary operator with p qubits.

$$H = H^\dagger = \frac{1}{\sqrt{2}} \begin{bmatrix} 1 & 1 \\ 1 & e^{\pi i} \end{bmatrix} = \frac{1}{\sqrt{2}} \begin{bmatrix} 1 & 1 \\ 1 & -1 \end{bmatrix} \quad (3)$$

$$iC-R_k^\dagger = \begin{bmatrix} 1 & 0 \\ 0 & e^{-2\pi i/2^k} \end{bmatrix} \quad (4)$$

A Quantum Phase Estimation (QPE) circuit consists of $n+p$ qubits. The first n *precision qubits* control the estimation accuracy, while the remaining p *phase qubits* encode the system state $|\psi\rangle$ whose phase is estimated. Controlled modular exponentiation operations ($C-U^{2^k}$) are applied to the phase qubits, followed by the inverse Quantum Fourier Transform (iQFT) on the precision qubits and final measurement. Ensuring functional correctness of QPE requires verifying each stage of the circuit, including superposition of the precision qubits, controlled modular exponentiation, iQFT, and measurement. Accordingly, our methodology proceeds in two steps: (i) verification of the precision qubits and (ii) verification of the phase qubits.

III. EXISTING APPROACHES

This section reviews work most closely related to our methodology. Hietala *et al.* [15] proposed SQIR, a Coq-based intermediate representation enabling machine-checked proofs of quantum algorithms such as QPE. SQIR verifies algorithmic specifications and supports extraction to executable languages (e.g., QASM [16], Qiskit [17]). However, it does not verify implemented circuits, requires substantial formalization (over 3,700 lines), and does not report scalability. In contrast, our approach verifies QPE implementations using only four concise properties and scales to 1,024 qubits with 6-bit precision. Chareton *et al.* [18] introduced Qbricks, a deductive verification framework based on symbolic path-sum semantics. While highly automated, scalability results are not reported. Our method instead applies abstraction to reduce quantum verification to bit-vector reasoning, enabling efficient and scalable verification of large QPE circuits. Peng *et al.* [19] presented a fully mechanized Coq verification of Shor’s algorithm using reversible circuits (RCIR). Although demonstrating end-to-end algorithmic correctness, the approach incurs significant formal effort and does not address scalability or verification of implemented circuits. Our methodology directly targets implemented QPE circuits [20], [21] and supports optimized designs while maintaining scalability. Several works apply formal verification to quantum circuits using equivalence checking [22], [23], path-sum representations [24], and theorem proving [25]. Unlike these approaches, our method does not require a golden

reference, avoids arithmetic overflow inherent to dyadic path-sum techniques, and offers superior scalability. We address these limitations and present a scalable formal verification of complete QPE circuits.

IV. ABSTRACTION FRAMEWORK

This section introduces the proposed abstraction framework by formally defining abstractions for qubits, gates, and operators. The framework exploits the fact that a global phase does not affect observable quantum behaviour [12]. Any qubit state can thus be expressed using a relative phase rotation on one basis state, as

$$|\psi\rangle = e^{\phi_1} \alpha |0\rangle + e^{\phi_2} \beta |1\rangle = e^{\phi_1} (\alpha |0\rangle + e^{\phi_2 - \phi_1} \beta |1\rangle). \quad (5)$$

Accordingly, our qubit abstraction retains only a single rotational component, capturing the relative phase term $e^{\phi_2 - \phi_1}$ as a rotation applied to $|1\rangle$. This representation can be decomposed into independent rotations on $|0\rangle$ and $|1\rangle$, denoted $r_{|0\rangle}$ and $r_{|1\rangle}$, following [11]. The framework further supports application-driven abstraction simplification. We next formalize the proposed qubit abstraction.

Definition 1. (*Abstract Qubit*) *The bit-vector abstraction Q of a qubit is a 4-tuple $\langle q, s, r, m \rangle$, where q, s, r , and m are bit-vectors of length 1, $\lceil \log_2(\max(H)+2) \rceil$, $n+p$, and 2, respectively.*

The abstract qubit consists of four components: the basis state q , the superposition component s , the rotational component r , and the measurement state m . The basis state q is encoded using a single bit since a qubit outside superposition lies in $\{0, 1\}$. The component s captures the superposition state of the qubit and tracks the number of Hadamard (H) gates applied to the qubit. Its length depends on the circuit and is determined by $\max(H)$, the maximum number of H gates on any qubit. This information is critical for verification, as an odd value of s indicates that the qubit is in superposition, and even, not. For example, in QPE, $\max(H) = 3$, yielding $\text{length}(s) = 3$.

The component r captures symbolic phase rotation and has length equal to the total number of qubits in the circuit. In QPE, phase accumulation from the inverse Quantum Fourier Transform (iQFT) can be represented as symbolic rotations applied to the $|1\rangle$ state. Phase induced by controlled modular exponentiation ($C-U^{2^k}$), reduced as relativistic phase rotations and are captured by symbolic rotations of r .

The abstraction of each quantum gate is defined next. The Hadamard (H) gate transforms an abstract qubit $\langle q^i, s^i, r^i, m^i \rangle$ to $\langle q^o, s^o, r^o, m^o \rangle$, where superscripts i and o denote input and output states.

Definition 2 (Abstract H Gate). [11] *If $s^i = \max(H) + 2$, then $s^o \leftarrow \max(H) + 1$; otherwise $s^o \leftarrow s^i + 1$. If $(s^i \text{ is even}) \wedge q^i = 1b0$, then $q^o = q^i$ and $r^o \leftarrow r^i$; else if $(s^i \text{ is even}) \wedge q^i = 1b1$, then $q^o = q^i$ and $r^o \leftarrow r^i +_n nb10 \dots 0$; else if $(s^i \text{ is odd}) \wedge q^i = 1b1$, then $q^o = r^i[n]$ and $r^o \leftarrow r^i -_n nb10 \dots 0$; else if $(s^i \text{ is odd}) \wedge q^i = 1b0$, then $q^o = r^i[n]$ and $r^o \leftarrow r^i$.*

Here, $+_n$ and $-_n$ denote fixed-point modular addition and subtraction with respect to n . Since QPE employs the iQFT,

the abstraction must support both QFT and iQFT. Accordingly, $\max(H) = 1$ for QFT and $\max(H) = 2$ for iQFT and QPE, yielding a superposition bit-vector of length three for QPE (Definition 1).

The H gate toggles s by incrementing it. For $\text{length}(s)=3$, $3b000, \dots, 3b111$. After $3b111$, value of s toggles between $3b110$ and $3b111$. Values exceeding $3b010$ in QPE indicate an error. Phase is captured by updating the rotational component r using modular arithmetic: entering superposition applies a clockwise rotation via $+_n nb10 \dots 0$, while exiting superposition applies an anti-clockwise rotation via $-_n nb10 \dots 0$. During superposition entry, $q^o = q^i$, and during exit, q^o is assigned the most significant bit of r^i . Since H is self-inverse ($H^\dagger = H$), the abstraction is valid in both directions. The H gate affects only q , s , and r , leaving the measurement component unchanged ($m^o = m^i$). The abstraction of the inverse controlled-rotation (C-R $_k^\dagger$) gate is presented next.

Definition 3. (*Abstract inverse Controlled-Rotation (C-R $_k^\dagger$) Gate*) [11] *If* $(q_c^i = 1b1 \wedge s_c^i = 3b010 \wedge s_t^i = 3b001)$, *then* $r_t^o \leftarrow r_t^i -_n \langle kb00 \dots 01_{k-n} 0 \dots 0 \rangle$, *else* $r_t^o \leftarrow r_t^i$, $q_t^o \leftarrow q_t^i$, $s_t^o \leftarrow s_t^i$.

Inverse controlled-rotation (C-R $_k^\dagger$) gates appear in the iQFT stage of QPE circuits. As per Definition 1, their abstraction uses a superposition bit-vector of length 3, derived from $\lceil \log_2(\max(H) + 2) \rceil$. The abstract C-R $_k^\dagger$ gate operates on a control qubit Q_c and a target qubit Q_t . When Q_c is in state $|1\rangle$ and not in superposition, and Q_t is in superposition, the gate induces an anti-clockwise phase rotation of $2\pi/2^k$ on Q_t . This effect is captured by modular subtraction from the rotational component r_t , encoding the rotation magnitude symbolically. In all other cases, the abstraction leaves the qubit state unchanged.

The C-R $_k^\dagger$ gate updates only the rotational component, while the basis, superposition, and measurement components remain unchanged. The corresponding clockwise controlled-rotation (C-R $_k$) gate is modelled analogously using modular addition, but is omitted here since QPE circuits employ only C-R $_k^\dagger$ gates. The abstraction of the controlled modular exponentiation (C-U $^{2^k}$) operation is presented next.

Definition 4. (*Abstract controlled-modular-exponentiation (C-U $^{2^k}$) Gate*) $\forall l \in \{1, 2, \dots, p\}$, *if* $q_c^i = 1b0$, *then* $r_{t_l}^o \leftarrow r_{t_l}^i$, *else if* $q_c^i = 1b1$, *then* $r_{t_l}^o \leftarrow r_{t_l}^i +_2 r_l \cdot \sum_{j=0}^k 2^j$, $k = \{0, 1, \dots, n-1\}$

In a QPE circuit, the controlled-modular-exponentiation operation applies powers of 2 to the unitary operator U , namely $U^{2^0}, \dots, U^{2^{n-1}}$, conditioned on the precision qubits. Within the abstraction framework, this behaviour is modelled as a symbolic phase rotation applied to the target qubits of U . If the control qubit (q_c) is in state $|0\rangle$, no update occurs. If q_c is in state $|1\rangle$, the rotational component of each target qubit (r_{t_l}) is updated via weighted modulo-2 addition, encoding the accumulated phase contribution of all powers of two ($r_{t_l}^o = r_{t_l}^i +_2 r_l \cdot 2^0 +_2 r_l \cdot 2^1 +_2 \dots +_2 r_l \cdot 2^{n-1}$). Here, r_{t_l} denotes the l^{th} qubit associated with the operator U , while $r_{t_l}^i$ and $r_{t_l}^o$ denote the rotation components of that qubit at the input and output, respectively. The abstraction updates only

the rotational component, while the basis, superposition, and measurement components remain unchanged.

Definition 5. (*Abstract Measurement (M-Gate)*) *If* $m^i = 2b00$, *then* $m^o = 2b01$; *elseif* $m^i = 2b01$, *then* $m^o = 2b10$; *elseif* $m^i = 2b10$, *then* $m^o = 2b11$; *elseif* $m^i = 2b11$, *then* $m^o = 2b10$.

The measurement abstraction tracks whether a qubit has been measured and enables detection of unintended or repeated measurements. A value $m = 2b00$ denotes an unmeasured qubit, while $m = 2b01$ represents a valid single measurement. All other values indicate multiple measurement events and are treated as errors (e.g., $m = 2b10$).

Together, these abstractions reduce quantum circuit verification from complex-valued Hilbert space to quantifier-free bit-vector space. The corresponding abstraction aligned correctness properties are defined next.

V. CORRECTNESS PROPERTIES

In this section, we give the abstraction-aligned correctness properties. The following convention is used for the abstract qubit components. The superscript represents the time evolution of qubit states and the subscript represents the qubit number. For example, $q_j^i, q_j^1, q_j^o, q_j^s$, represents the basis state component at input, first, stage before output and at the output respectively for the j^{th} qubit. Similarly for all other components s, r , and m .

Property 1. (*Superposition Correctness*) $\forall Q_1, Q_2, \dots, Q_n$ *in precision block of QPE circuit*, $(s_1^i = 3b000 \wedge s_2^i = 3b000 \wedge \dots \wedge s_n^i = 3b000) \rightarrow (s_1^1 = 3b001 \wedge s_2^1 = 3b001 \wedge \dots \wedge s_n^1 = 3b001) \wedge (s_1^o = 3b010 \wedge s_2^o = 3b010 \wedge \dots \wedge s_n^o = 3b010)$. *And*, $\forall Q_1, Q_2, \dots, Q_p$ *in phase block of QPE circuit*, $(s^o = s^i)$

This property ensures that qubit superposition evolves correctly. Precision qubits start outside superposition ($s^i = 3b000$). The initial H -gate creates superposition ($s^1 = 3b001$), and the inverse QFT (iQFT) returns them to a non-superposition state ($s^o = 3b010$), consistent with $H^\dagger = H$. Phase qubits are only affected by controlled modular exponentiation (C-U $^{2^k}$), which leaves their superposition unchanged. Hence, for all phase qubits, $s^o = s^i$, ensuring superposition correctness across the QPE circuit.

Property 2. (*iQFT Correctness*) $\langle (\forall b_1, b_2, \dots, b_n \in \{1b0, 1b1\}: \bigwedge_{j=1}^n (r_j^1 = nb b_j b_{j+1} \dots b_n 0 \dots 0 \wedge s_j^1 = 3b001) \rightarrow (\bigwedge_{j=1}^n r_j^o = nb00 \dots 0 \wedge q_j^o = b_j)) \rangle$.

This property verifies the correctness of the iQFT block in QPE [11]. The iQFT reverses the rotations applied during the QFT, restoring the qubits to their original states. Formally, if the j^{th} input qubit has rotational component $r_j^i = nb b_j b_{j+1} \dots b_n 0 \dots 0$ with superposition $s = 3b001$, then after iQFT, the rotation is reset to $r_j^o = nb00 \dots 0$, and the output basis state matches $q_j^o = b_j$. This guarantees that the inverse transformation correctly recovers the encoded bit-vector state for all precision qubits.

Property 3. (*Measurement Correctness*) $(m_1^i = 2b00 \wedge m_2^i = 2b00 \wedge \dots \wedge m_n^i = 2b00) \wedge (m_p^i = 2b00) \rightarrow (m_1^o = 2b00$

$$\wedge m_2^o=2b00 \wedge \dots \wedge m_n^o=2b00) \wedge (m_1^o=2b01 \wedge m_2^o=2b01 \wedge \dots \wedge m_n^o=2b01) \wedge (m_p^i=2b00)$$

This property ensures correct measurement behaviour in QPE. Precision qubits must remain unmeasured throughout the circuit until the final output stage: $m_1^i = \dots = m_n^i = 2b00$ and $m_1^o = \dots = m_n^o = 2b00$. At the output, each precision qubit is measured exactly once, $m_1^o = \dots = m_n^o = 2b01$. Phase qubits are not measured, maintaining $m_p^i = m_p^o = 2b00$. This guarantees that measurements occur only at the designated output stage, preventing redundant or premature measurement operations.

Property 4. (Phase Qubit Correctness) $\forall Q_1, Q_2, \dots, Q_n$ in precision block and $Q_{p_1}, Q_{p_2}, \dots, Q_{p_p}$ in the phase block of QPE, the following should hold:

$$\begin{aligned} (r_{p_1}^o = q_1 \cdot r_1 + q_2 \cdot (2r_1) + q_3 \cdot (4r_1) + \dots + q_n \cdot (2^{n-1}r_1)) \wedge \\ (r_{p_2}^o = q_1 \cdot r_2 + q_2 \cdot (2r_2) + q_3 \cdot (4r_2) + \dots + q_n \cdot (2^{n-1}r_2)) \wedge \\ \vdots \end{aligned}$$

$(r_{p_p}^o = q_1 \cdot r_p + q_2 \cdot (2r_p) + q_3 \cdot (4r_p) + \dots + q_n \cdot (2^{n-1}r_p))$, where r_1, r_2, \dots, r_p are the symbolic rotations applied by the unitary operator U on qubit $Q_{p_1}, Q_{p_2}, \dots, Q_{p_p}$ respectively.

Property 4 ensures the functional correctness of the phase block in QPE. Let r_1, \dots, r_p denote the symbolic rotations applied by U as a result of $C-U^{2^k}$ operations on the phase qubits Q_{p_1}, \dots, Q_{p_p} , with outputs $r_{p_1}^o, \dots, r_{p_p}^o$. A rotation is applied to Q_{p_k} only when the corresponding control qubit Q_j is in $|1\rangle$, represented as $q_j \cdot r_{p_k}$. Controlled modular exponentiation ($C-U^{2^k}$) is thus abstracted as weighted rotations $q_j \cdot 2^j \cdot r_k$, accumulated modulo arithmetic on each phase qubit. Here, we assume that the input qubit has no rotation component in the phase block, i.e., $r_{t_i}^i = 0$ (Definition 4). All phase qubits must satisfy these conditions to guarantee correct phase rotation in the QPE circuit.

VI. VERIFICATION METHODOLOGY

As discussed in Section II, our verification methodology proceeds in two steps: (i) precision qubit verification, and (ii) phase qubit verification. Figure 1(c) illustrates a QPE circuit with three precision qubits (q_0, q_1, q_2) and one phase qubit (q_3), implemented in IBM Qiskit [17]. Modular exponentiation is realized by applying $C-U^{2^i}$, 2^i times on the phase qubit for each precision qubit $i \in \{0, 1, 2\}$.

The circuit is first abstracted from Hilbert space to the bit-vector domain (Section IV) and encoded into SMT form. Verification is performed using the Z3 solver [26], leveraging the four correctness properties. Properties 1-3 validate superposition, iQFT, and measurement correctness, while Property 4 ensures correct phase-qubit rotation under $C-U^{2^k}$. We evaluate scalability on QPE circuits with up to 6 precision qubits and $C-U^{2^k}$ operators spanning up to 1,024 qubits.

Typical QPE errors include: (i) superposition errors from missing or extra H/H^\dagger gates, (ii) iQFT errors from incorrect parameters in $C-R_k^\dagger$ gates, (iii) measurement errors such as missing, extra, or unintended measurements, and (iv) incorrect controlled modular exponentiation due to wrong control or

target qubits. Verification of the unitary operator itself is application dependent and not covered here. We assume correct state preparation and unitary implementation. The following lemmas demonstrate that any of these errors violate one or more correctness properties, enabling their detection.

Lemma 1. *In a QPE circuit, applying zero or more than one H-gate (or H^\dagger -gate) on a precision qubit, or any H-gate on a phase qubit, violates Property 1.*

Proof. Consider a qubit Q_j . Property 1 enforces that for a precision qubit, $s_j^i = 3b000$ at input and $s_j^o = 3b010$ at output, corresponding to two H-gate applications: one to create superposition and one in the iQFT. For phase qubits, $s_j^i = s_j^o = 3b000$.

Case 1: No H-gate on a precision qubit:

If no H-gate is applied, s_j remains $3b000$ at output (Definition 2), violating the required $s_j^o=3b010$.

Case 2: More than one H-gate on a precision qubit:

By Definition 2, s_j increments by $3b001$ per H-gate. Applying three or more H-gates yields $s_j^o \neq 3b010$ (e.g., $3b011$ or higher), violating Property 1.

Case 3: H-gates on a phase qubit:

If any H-gate is applied to a phase qubit, s_j changes from $3b000$, violating the requirement $s_j^o=3b000$.

In all cases, Property 1 is violated. As $H=H^\dagger$, the proof holds for both. \square

Lemma 2. *If any H^\dagger -gate in the iQFT block of a QPE circuit is omitted, applied multiple times on the same qubit, or applied at an incorrect position, then either Property 1 or Property 2 or both are violated.*

Proof. Let Q_j denote the j^{th} qubit in the iQFT block. Assuming the input qubit to iQFT is already in superposition, Property 1 requires

$$s_j^i = 3b001, \quad s_j^o = 3b010. \quad (6)$$

Case 1: Omission of H^\dagger .

If H^\dagger is not applied, then $s_j^o = 3b001 \neq 3b010$, violating Property 1.

Case 2: Multiple H^\dagger gates.

Applying more than one H^\dagger gate yields $s_j^o \neq 3b010$, again violating Property 1.

Case 3: Incorrect placement of H^\dagger .

Let Q_c and Q_t be the control and target of a $C-R_k^\dagger$ gate. By Definition 3, for control (Q_c) and target qubit (Q_t),

$$s_c^i = 3b010, \quad s_t^i = 3b001. \quad (7)$$

If H^\dagger is mispositioned, either $s_c^i \neq 3b010$ or $s_t^i \neq 3b001$, which results in

$$r_j^o \neq \langle nb00 \dots 0 \rangle, \quad (8)$$

violating Property 2.

Thus, any error in H^\dagger gates affects either s or r of the abstract qubit, ensuring that Property 1 or Property 2 is violated. \square

Lemma 3. *If the rotation applied by any $C-R_k^\dagger$ gate is incorrect due to misplacement, wrong control, or wrong target qubit, Property 2 is violated.*

Proof. Let Q_j be a precision qubit. Property 2 requires

$$r_j^o = nb00\dots 0, \text{ and } q_j^o = b_j. \quad (9)$$

Case 1: Missing $C-R_k^\dagger$ gate.

Without the gate, the intended anti-clockwise rotation on r_j is not applied, giving $r_j^o \neq nb00\dots 0$, violating Property 2.

Case 2: Extra $C-R_k^\dagger$ gates.

Additional gates cause over-rotation, again yielding $r_j^o \neq nb00\dots 0$, violating Property 2.

Case 3: Incorrect control or target qubit.

Suppose an $C-R_k^\dagger$ gate uses bit b_q in place of the intended bit b_p as the control (or target). The phase rotation applied becomes

$$2\pi \left(\frac{b_q}{2} + \frac{b_{q+1}}{4} + \dots + \frac{b_m}{2^{m-q}} \right)$$

instead of the correct

$$2\pi \left(\frac{b_p}{2} + \frac{b_{p+1}}{4} + \dots + \frac{b_m}{2^{m-p}} \right).$$

This mismatch in applied phase rotation in all cases where $q \neq p$ yields

$$r_j^o \neq nb00\dots 0, \quad (10)$$

This violates the precise rotation condition enforced by Property 2. Thus, any deviation in count, placement, or qubit assignment of $C-R_k^\dagger$ gates modifies r , causing Property 2 to fail. \square

Lemma 4. *Any error in the measurement operation violates Property 3.*

Proof. Consider the measurement components of a precision qubit Q_k (m_k) and a phase qubit Q_j (m_j), with $k \in \{1, \dots, n\}$ and $j \in \{1, \dots, p\}$. Property 3 requires:

- 1) Input measurements: $m_k^i = 2b00$ for precision qubits and $m_j^i = 2b00$ for phase qubits.
- 2) Intermediate stages till before measurement: $m_k^o = 2b00$.
- 3) Final output: $m_k^o = 2b01$ for precision qubits, $m_j^o = 2b00$ for phase qubits.

Case 1: Extra measurement on a precision qubit.

If a measurement occurs before the output stage, then by Definition 5, at some intermediate stage x , $m_k^x \neq 2b00$ violating Property 3.

Case 2: Missing measurement on a precision qubit.

If the output measurement is absent, $m_k^o = 2b01 \neq 2b01$, violating Property 3.

Case 3: Accidental measurement of a phase qubit.

If Q_j is measured, $m_j^o \neq 2b00$, violating Property 3.

Thus, any deviation in measurement operations causes Property 3 to be violated. \square

Lemma 5. *Any error in the controlled-modular-exponentiation ($C-U^{2^k}$) operation, such as incorrect control or target assignment, results in an incorrect symbolic rotation on the phase qubit, violating Property 4.*

Proof. Let Q_j be a control (precision) qubit and Q_{p_k} a phase qubit. By Property 4, the correct rotational update is:

$$r_{p_k}^o = r_{p_k}^i + \sum_{j=0}^{n-1} 2^j q_j r_{p_k}, \quad (11)$$

where $q_j \in \{0, 1\}$ is the control qubit basis and $r_{p_k}^i, r_{p_k}^o$ are input, and output rotations respectively of phase qubits.

Case 1: Incorrect control assignment.

If a wrong control $q_{j'}$ is used, the output becomes

$$\tilde{r}_{p_k}^o = r_{p_k}^i + \sum_{t \neq j} 2^t q_t r_{p_k} + 2^j q_{j'} r_{p_k} \neq r_{p_k}^o, \quad (12)$$

violating Property 4.

Case 2: Incorrect target assignment.

If the rotation intended for Q_{p_k} is applied to $Q_{p_{k'}}$ ($k' \neq k$), then

$$\tilde{r}_{p_k}^o = r_{p_k}^i, \quad \tilde{r}_{p_{k'}}^o = r_{p_{k'}}^i + \sum_{j=0}^{n-1} 2^j q_j r_{p_k}, \quad (13)$$

so Q_{p_k} fails the required rotation, violating Property 4.

Hence, any incorrect control or target assignment in $C-U^{2^k}$ leads to an incorrect symbolic rotation, causing Property 4 to be violated. \square

Lemma 6. *Any combination of errors described in Lemmas 1–5 in a QPE circuit will violate at least one of Properties 1–4 during verification.*

Proof. Each error type in Lemmas 1–5 is independently detectable by the corresponding property. Since the verification framework monitors all four properties, any combination of errors triggers at least one property violation. Thus, multiple concurrent errors are detected, guaranteeing that at least one of Properties 1–4 is violated. \square

Theorem 1. *If the abstracted QPE circuit satisfies Properties 1–4, the corresponding quantum circuit correctly implements the Quantum Phase Estimation algorithm.*

Proof. Errors in a QPE circuit can arise from Hadamard (H) gates, inverse controlled-rotation ($C-R_k^\dagger$) gates, controlled-modular-exponentiation ($C-U^{2^k}$) operations, or measurement operations. Properties 1–2 ensure the functional correctness of precision qubits, including proper application of H and $C-R_k^\dagger$ gates. Property 3 guarantees correct measurement, and Property 4 ensures accurate phase accumulation on the phase qubits via $C-U^{2^k}$. Together, these properties cover all error scenarios outlined in Lemmas 1–5. By Lemma 6, any combination of such errors violates at least one property. Hence, if all Properties 1–4 hold on the abstracted model, no errors are present, and the original quantum circuit faithfully implements QPE. \square

VII. EXPERIMENTAL RESULTS

This section presents the verification benchmarking results. All experiments were performed on a system with an Intel® Core™ Ultra 9 285K CPU at 3.2 GHz, 192 GB RAM, running RHEL 9 (64-bit), using Z3 SMT solver v4.8.12. Verification proceeds in two stages as described in Section VI. The iQFT stage is verified using the method in [11]. For a 6-qubit precision configuration, verification completes in 0.01 s with peak memory of 17 MB. A 6-bit precision provides phase accuracy up to $1/2^6$. Table I summarizes results for 6-bit

TABLE I
PHASE BLOCK VERIFICATION RESULTS

Circuit Benchmark Phase Qubits Count	Correct Circuit		Error Circuit	
	Time(s)	Memory(MB)	Time(s)	Memory(MB)
2	0.33	27.4	0.03	27.4
4	0.91	29.1	0.09	29.1
8	1.91	40.7	0.09	40.74
16	7.42	80.3	0.41	80.3
32	45.73	149	1.10	150
64	196	243	0.80	292
128	1,407	480	15.4	481
256	10,524	1,108	142	872
512	64,383	3,109	8.05	1,717
1,024	288,196	7,663	15.9	3,434

precision circuits with phase-qubit counts from 2 to 1,024. The *Phase Qubits Count* column indicates the number of phase qubits. *Time (s)* and *Memory (MB)* report total verification time and peak memory, respectively. *Correct Circuit* corresponds to error-free $C-U^{2^k}$ implementations, while the *Error* columns show results for injected control-qubit errors at the first qubit. Other error scenarios are verified and consume fewer resources than correct circuit and are omitted from reporting for brevity.. As observed, verification time for larger circuits with errors (512, 1024 qubits) is lower despite higher memory usage, due to internal Boolean optimizations in Z3.

VIII. CONCLUSION AND FUTURE WORKS

We demonstrated a symbolic abstraction framework using quantifier-free bit-vector logic to model qubits, quantum gates, and operators, extending the abstraction to include measurement along with rotation and superposition. This framework reduces the verification of Quantum Phase Estimation (QPE) circuits from the complex-valued Hilbert space to a bit-vector domain. We define formal correctness properties capturing the functional behaviour of QPE circuits and lemmas covering key error scenarios, ensuring that all such errors are detectable. Experimental results demonstrate scalability, successfully verifying QPE circuits with up to 1,024 phase qubits in the unitary operator and 6-bit precision qubits. Future work will focus on reducing verification time for larger circuits and extending the framework to formally verify concrete unitary operators, enabling analysis of more complex quantum algorithms.

REFERENCES

- [1] V. Hassija, V. Chamola, A. Goyal, S. S. Kanhere, and N. Guizani, "Forthcoming applications of quantum computing: peeking into the future," *IET Quantum Communication*, vol. 1, no. 2, pp. 35–41, 2020.
- [2] G. Arun and V. Mishra, "A review on quantum computing and communication," in *2014 2nd International Conference on Emerging Technology Trends in Electronics, Communication and Networking*, 2014, pp. 1–5.
- [3] G. Carrascal, P. Hernamperez, G. Botella, and A. d. Barrio, "Backtesting quantum computing algorithms for portfolio optimization," *IEEE Transactions on Quantum Engineering*, vol. 5, pp. 1–20, 2024.
- [4] P. W. Shor, "Polynomial-time algorithms for prime factorization and discrete logarithms on a quantum computer," *SIAM Review*, vol. 41, no. 2, pp. 303–332, 1999.
- [5] G. Brassard, P. Høyer, and A. Tapp, *Quantum counting*, 1998, pp. 820–831.
- [6] R. D. Somma, "Quantum eigenvalue estimation via time series analysis," *New Journal of Physics*, vol. 21, p. 123025, 12 2019.
- [7] A. W. Harrow, A. Hassidim, and S. Lloyd, "Quantum algorithm for linear systems of equations," *Physical Review Letters*, vol. 103, p. 150502, 10 2009.
- [8] O. Hasan and S. Tahar, "Formal verification methods," in *Encyclopedia of Information Science and Technology, Third Edition*. IGI global, 2015, pp. 7162–7170.
- [9] C. Charetton, S. Bardin, D. Lee, B. Valiron, R. Vilmart, and Z. Xu, "Formal methods for quantum programs: A survey," 2022.
- [10] A. Govindankutty, "A review of formal methods in quantum-circuit verification," *Electronics*, vol. 15, no. 5, 2026.
- [11] G. Arun, S. Srinivasan, and Y. Moshood, "Verification of quantum fourier transform and its inverse via rotational and superposition abstraction," in *IEEE International Symposium on Circuits and Systems*, 2026.
- [12] M. A. Nielsen and I. L. Chuang, *Quantum Computation and Quantum Information: 10th Anniversary Edition*, 10th ed. USA: Cambridge University Press, 2011.
- [13] C. Bernhardt, *Quantum Computing for Everyone*. MIT Press, 2020.
- [14] R. LaPierre, *Introduction to Quantum Computing*. Springer International Publishing, 2021.
- [15] K. Hietala, R. Rand, S.-H. Hung, L. Li, and M. Hicks, "Proving Quantum Programs Correct," in *12th International Conference on Interactive Theorem Proving (ITP 2021)*, ser. Leibniz International Proceedings in Informatics (LIPIcs), L. Cohen and C. Kaliszyk, Eds., vol. 193. Dagstuhl, Germany: Schloss Dagstuhl – Leibniz-Zentrum für Informatik, 2021, pp. 21:1–21:19.
- [16] A. Cross, A. Javadi-Abhari, T. Alexander, N. D. Beaudrap, L. S. Bishop, S. Heidel, C. A. Ryan, P. Sivarajah, J. Smolin, J. M. Gambetta, and B. R. Johnson, "Openqasm 3: A broader and deeper quantum assembly language," *ACM Transactions on Quantum Computing*, vol. 3, pp. 1–50, 9 2022.
- [17] A. Javadi-Abhari, M. Treinish, K. Krsulich, C. J. Wood, J. Lishman, J. Gacon, S. Martiel, P. D. Nation, L. S. Bishop, A. W. Cross, B. R. Johnson, and J. M. Gambetta, "Quantum computing with qiskit," 2024.
- [18] C. Charetton, S. Bardin, F. Bobot, V. Perrelle, and B. Valiron, *An Automated Deductive Verification Framework for Circuit-building Quantum Programs*, 2021, pp. 148–177.
- [19] Y. Peng, K. Hietala, R. Tao, L. Li, R. Rand, M. Hicks, and X. Wu, "A formally certified end-to-end implementation of shor's factorization algorithm," *Proceedings of the National Academy of Sciences*, vol. 120, 5 2023.
- [20] A. Govindankutty, S. K. Srinivasan, and N. Mathure, "Rotational abstractions for verification of quantum fourier transform circuits," *IET Quantum Communication*, vol. 4, no. 2, pp. 84–92, 2023.
- [21] A. Govindankutty and S. K. Srinivasan, "Superposition-based abstractions for quantum data encoding verification," *IET Quantum Communication*, vol. 6, no. 1, p. e70002, 2025.
- [22] S. Yamashita and I. L. Markov, "Fast equivalence-checking for quantum circuits," *Quantum Info. Comput.*, vol. 10, no. 9, p. 721–734, Sep. 2010.
- [23] Y. Feng, N. Yu, and M. Ying, "Model checking quantum markov chains," *Journal of Computer and System Sciences*, vol. 79, no. 7, pp. 1181–1198, 2013.
- [24] M. Amy, "Towards large-scale functional verification of universal quantum circuits," *Electronic Proceedings in Theoretical Computer Science*, vol. 287, pp. 1–21, 1 2019.
- [25] J. Liu, B. Zhan, S. Wang, S. Ying, T. Liu, Y. Li, M. Ying, and N. Zhan, "Formal verification of quantum algorithms using quantum hoare logic," in *Computer Aided Verification*, I. Dillig and S. Tasiran, Eds. Cham: Springer International Publishing, 2019, pp. 187–207.
- [26] L. De Moura and N. Bjørner, "Z3: An efficient smt solver," in *Proceedings of the Theory and Practice of Software, 14th International Conference on Tools and Algorithms for the Construction and Analysis of Systems*, ser. TACAS'08/ETAPS'08. Berlin, Heidelberg: Springer-Verlag, 2008, p. 337–340.